Blinking suppression and biexcitonic emission in thick-shell CdSe/CdS nanocrystals at cryogenic temperature

D Canneson, L Biadala, S Buil, Xavier Quélin, C Javaux, B Dubertret, J.-P Hermier

▶ **To cite this version:**

D Canneson, L Biadala, S Buil, Xavier Quélin, C Javaux, et al.. Blinking suppression and biexcitonic emission in thick-shell CdSe/CdS nanocrystals at cryogenic temperature. Physical Review B: Condensed Matter and Materials Physics (1998-2015), American Physical Society, 2014, 10.1103/PhysRevB.89.035303 . hal-01340738

HAL Id: hal-01340738
https://hal.uvsq.fr/hal-01340738

Submitted on 1 Jul 2016

HAL is a multi-disciplinary open access archive for the deposit and dissemination of scientific research documents, whether they are published or not. The documents may come from teaching and research institutions in France or abroad, or from public or private research centers.

L'archive ouverte pluridisciplinaire **HAL**, est destinée au dépôt et à la diffusion de documents scientifiques de niveau recherche, publiés ou non, émanant des établissements d'enseignement et de recherche français ou étrangers, des laboratoires publics ou privés.

Blinking suppression and biexcitonic emission in thick-shell CdSe/CdS nanocrystals at cryogenic temperature

D. Canneson,[1] L. Biadala,[1] S. Buil,[1] X. Quélin,[1] C. Javaux,[2] B. Dubertret,[2,*] and J.-P. Hermier[1,3,†]

[1]*Groupe d'Étude de la Matière Condensée, Université de Versailles-Saint-Quentin-en-Yvelines, Centre National de la Recherche Scientifique UMR8635, 45 Avenue des États-Unis, 78035 Versailles, France*

[2]*Laboratoire de Physique et d'Étude des Matériaux, Centre National de la Recherche Scientifique UMR8213, École Supérieure de Physique et de Chimie Industrielles de la Ville de Paris, 10 Rue Vauquelin, 75231 Paris, France*

[3]*Institut Universitaire de France, 103 Boulevard Saint-Michel, 75005 Paris, France*

(Received 14 September 2013; revised manuscript received 25 November 2013; published 9 January 2014)

The fluorescence of single colloidal thick-shell CdSe/CdS nanocrystals (NCs), at cryogenic temperature (4 K) and room temperature (RT), is studied using the intensity autocorrelation function (ACF) and lifetime measurements. The radiative and Auger decay rates corresponding to the desexcitation of the charged biexcitonic state are determined through an original method of photon postselection. Especially, the charged biexciton quantum yield increases from about 15% at RT to 60% at 4 K. The high inhibition of Auger recombination already observed for the trion state of CdSe/CdS NCs at low temperature is also demonstrated for the charged biexcitonic state. At 4 K, the ACF is equal to 1 for time scales ranging from 50 ns to 200 ms. In contrast with RT operation, the intensity of the trion emission is then perfectly stable and no blinking is observed. All the results highlight the strong confinement of the charge carriers in the CdSe core.

DOI: 10.1103/PhysRevB.89.035303 PACS number(s): 78.67.Bf, 42.50.Ar, 78.55.Cr, 79.20.Fv

I. INTRODUCTION

Recently, CdSe NCs with a thick (more than 5 nm) CdS shell have been synthesized.[1,2] At the single molecule level, the fluorescence emission of these structures fluctuates in intensity but a complete dark state is never reached. Even if blinking properties of nanocrystals (NCs) are complex phenomena[3,4] that cannot be solely explained by a fast Auger recombination in charged NCs[5] and may involve multiple recombination centers,[6,7] it was shown that the blinking inhibition in CdSe/CdS NCs resulted from a reduction of the Auger recombination efficiency. While in regular CdSe/ZnS NCs the Auger lifetime scales as the volume of the emitter and is usually of the order of 10–100 ps,[8,9] in the case of thick-shell CdSe/CdS NCs, Auger lifetimes in the range of tens of nanoseconds have been measured.[10–12] Strongly suppressed Auger recombinations have also been observed in other core/shell structures,[13,14] and recently gray states have been also reported for CdSe/ZnS NCs.[15] It is well known that fast Auger processes result in photon antibunching[16,17] and biexciton emission is hardly observed in regular NCs.[18–21] The efficiency of Auger recombinations also severely limits the use of colloidal NCs in lasing applications.[22] As a consequence, several groups actively investigate both theoretical[23,24] and experimental methods to obtain colloidal NCs with completely suppressed Auger processes.[11,19,20,25,26]

In a recent paper,[27] the thermal activation of nonradiative Auger recombination was demonstrated for the negative trion state X^*. As a result, the X^* emission is stable,[28] with a quantum yield (QY) increasing continuously when decreasing the temperature. It is close to 100% under 30 K. A theoretical analysis[27,29] suggests that the thermal activation of Auger recombination for the negative trion state comes from the delocalization of one of the electrons from the CdSe core into the CdS shell. This electron probes the abrupt potential at the NC surface, that leads to the nonradiative Auger recombination.

In this paper, the modifications of the CdSe/CdS NC fluorescence between 4 K and room temperature (RT) are investigated in detail through the autocorrelation function (ACF) of the intensity, also mentioned as $g^{(2)}(\tau)$. First, using the value of the ACF at zero delay, the thermal activation of Auger processes is evidenced for the negatively charged biexcitonic BX^* state. Measurements were performed for both the charged biexciton lifetime and QY at RT and at 4 K. We found that the BX^* QY increases from 15% at RT to 60% at 4 K, showing a thermal activation of Auger processes for the BX^* state. A postselection of the photons also provides all the decay rates involved in the desexcitation of BX^*. These results can be explained by the strong confinement of the charge carriers for BX^*, analogous to the one demonstrated for X^*.[27] In a second step, the ACF for positive delays ranging on a time scale of more than five orders of magnitude (from less than 1 μs to 200 ms) is used to compare the intensity fluctuations of the trion state at RT and 4 K. While bunching corresponding to blinking is observed at RT, the ACF is equal to 1 at 4 K. The trion of a CdSe/CdS NC is then a perfect emitting state with no QY fluctuations.

II. EXPERIMENTAL SETUP

CdSe/CdS core-shell NCs with a 2.5-nm core radius and a 6-nm-thick shell were synthesized using a modification of the method described in Ref. 2. Their emission is centered around 660 nm with a full width at half maximum of about 30 nm. The nanoparticles were suspended in a mixture of 90% hexane and 10% octane and spin coated on a glass coverslip in such a way that single NCs could be observed with an epifluorescent microscope (IX 71, Olympus) at the single molecule level. At 4 K, the coverslip was mounted in a continuous flow helium cryostat (Microstat-He HiRes, Oxford Instruments). The NCs were excited with a laser diode emitting at 405 nm (LDH-P-C-405, Picoquant, pulse duration ~100 ps, repetition rate of

 ©2014 American Physical Society

2.5 MHz at RT and 20 MHz at 4 K). The pump excitation is weak: the probability to create n electron-hole pairs follows a Poissonian statistics[12] with a mean value lower than 0.3. The emission was collected by an objective with a 1.4 numerical aperture (RT) or a 0.7 numerical aperture (4 K) and analyzed with a Hanbury-Brown and Twiss setup. The photodetection signals were sent into a PicoHarp 300 module (Picoquant) that gives the absolute time for each photodetection event (time resolution of 300 ps). The data from a single record provide the fluorescence intensity versus time, the histogram of the delays between photons at a time scale only limited by the duration of the experiment and the photoluminescence (PL) decay. From a very general point of view, using a single set of data offers the possibility to apply postselection approaches.[30] When biexcitonic cascades are detected, in contrast with a standard Hanbury-Brown and Twiss setup that only gives the delay between photons, the photons corresponding to biexcitonic and monoexcitonic emission can be selected and the decay rates of the two states can be deduced.

III. FLUORESCENCE PROPERTIES OF SINGLE CDSE/CDS NCS AT 4 K

A. Preliminary results

In air and at RT [Fig. 1(a)], the fluorescence intensity versus time of a single NC switches between two values corresponding to a bright (monoexciton X) and a gray (trion X*) state. The X state exhibits a near unity QY while the X* state radiative QY ($Q_{X^*}^{\mathrm{RT}}$) is about 40%.[12,27] The PL decay is well fitted by a biexponential curve with a long component ($\geqslant \tau_b = 60$ ns) that corresponds to the X state while the short component ($\sim \tau_g = 10$ ns) corresponds to the X* state.[31]

As recently shown,[27] a CdSe/CdS NC is always ionized at 4 K. The QY of the trion state under 30 K is also close to 100% and its lifetime is about 8 ns. In contrast to CdSe/CdS NCs at RT, the Auger recombination of X* is not observed. From 30 to 300 K, it was found that the Auger lifetime decreases from a nonmeasurable value to a typical value of 20 ns.

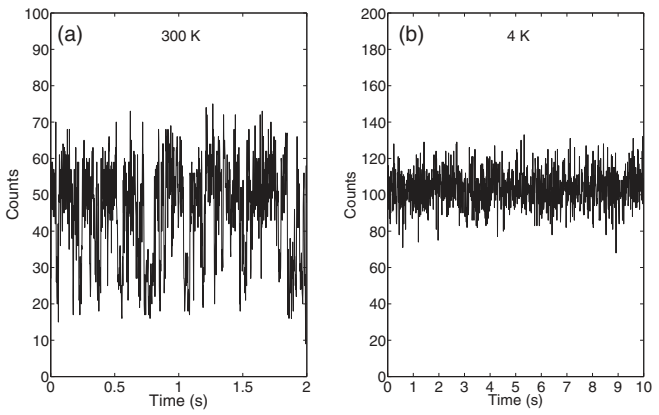

FIG. 1. (a) Fluorescence intensity trace of a single NC at RT in air (time bin = 2 ms, dark counts = 0.4 per 2 ms). (b) Fluorescence intensity trace of a single NC at 4 K (time bin = 10 ms, dark counts = 15 per 10 ms).

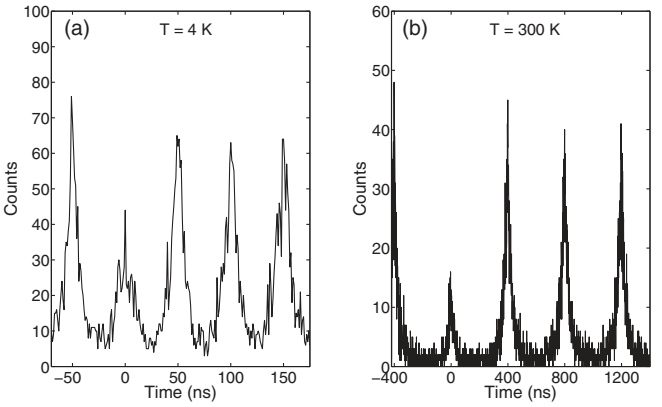

FIG. 2. (a) Coincidence counts at 4 K. The area of the peak at zero delay is 60% of the mean area of the lateral peaks (after background correction). (b) Coincidence counts of the emission of another NC when it is in an ionized state at RT. The area of the peak at zero delay is then 40% of the mean area of the lateral peaks (after background correction).

B. Biexcitonic emission

The consequence of thermal Auger activation is now analyzed for the biexcitonic state BX* recombination. The QY is notably determined both at 4 K and at RT. This analysis is done using a method based on the intensity autocorrelation measurement presented in detail in Ref. 32. Figure 2(a) shows a typical coincidences histogram at short delays at 4 K. The peak at zero delay has an area equal to 60% of the mean area of the lateral peaks. Under low pump excitation, this value corresponds to the ratio between the radiative QY of the BX* state and the radiative QY of the X* state. Since the X* state has a near unity QY at 4 K, the BX* QY at 4 K ($Q_{\mathrm{BX}^*}^{\mathrm{4K}}$) is directly found to be 60%.

We now characterize the BX* QY at RT. The analysis is less straightforward since the NC oscillates between X* and X states in air. The photons corresponding to the X* state can be selected using a postacquisition intensity threshold.[12] For these photons, the histogram of the delays between photons [Fig. 2(b)] was calculated. The area of the peak at zero delay is typically about 40% of the mean area of the lateral peaks. Since the X* QY is ~40% at RT, the QY of the BX* at room temperature is of the order of 40% × 40%, which is approximately 15%. The BX* QY at 4 K is thus four times greater than the one at RT. This value does not depend on the NC.

In the peak at delays close to zero [Figs. 2(a) and 2(b)], coincidences correspond to the detection of a two-photon cascade: the first detection event is due to a radiative recombination of BX* while the second event corresponds to the photons generated by the desexcitation of X*. Since the delay between the laser pulse and each collected photon is recorded, the photons stemming from BX* and the ones stemming from X* can be tagged unambiguously.[30] In Fig. 3, the corresponding PL decays for X* [Fig. 3(a)] and BX* [Fig. 3(b)] states are plotted. These curves are perfectly fitted by a monoexponential decay. From these fits, we obtain the lifetime of X* (6.1 ns) and BX* (1.5 ns). These values are confirmed by a very satisfying bi-exponential fit of the total PL decay with components of 1.5 and 5.7 ns [Fig. 3(c)]. The total decay rate of the BX* state

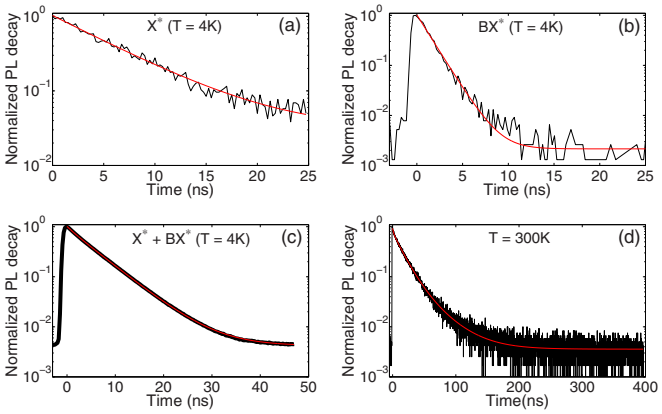

FIG. 3. (Color online) (a) PL decay corresponding to X* recombination. The photons are selected from the peak at zero delay [see Fig. 2(a)]. The red line is a monoexponential decay (with an offset, lifetime of 6.1 ns). (b) PL decay corresponding to BX* recombination. The photons are selected from the peak at zero delay of Fig. 2(a). The red line is a monoexponential decay (with an offset, lifetime of 1.5 ns). (c) Total PL decay. The red line is a biexponential decay (with an offset, lifetime of 1.5 and 5.7 ns). (d) PL decay corresponding to X* recombination at RT (the photons are postselected using a threshold intensity as in Fig. 2). The red line is a triexponential decay [with an offset, lifetimes of 1.5 ns (17%), 15 ns (68%), and 36 ns (15%)]. The first component corresponds to the BX* state, and the second one corresponds to the X* state. The last component corresponds to residual photons of the X state that have not been filtered. The discrepancy between the value of 36 ns and the X lifetime, greater than 60 ns, comes from the low number of photons corresponding to the recombination of the X state.

$k_{BX^*}^{4K}$ is the sum of the radiative decay rate $k_{BX^*}^{rad,4K}$ and the Auger decay rate $k_{BX^*}^{Auger,4K}$. Since $Q_{BX^*}^{4K} = 60\%$ is given by

$$Q_{BX^*}^{4K} = \frac{k_{BX^*}^{rad,4K}}{\left(k_{BX^*}^{rad,4K} + k_{BX^*}^{Auger,4K}\right)}, \quad (1)$$

all the decay rates can be calculated. One finds that $k_{BX^*}^{rad,4K} = 1/2.5\ ns^{-1}$ and $k_{BX^*}^{Auger,4K} = 1/3.8\ ns^{-1}$. In principle, the same method could be applied at room temperature. However, the X* QY as well as the one of BX* are much lower at room temperature. Taking into account the ratios $Q_{BX^*}^{4K}/Q_{BX^*}^{RT} \sim 4$ and $Q_{X^*}^{4K}/Q_{X^*}^{RT} \sim 2.5$, the experimental time needed to record the same number of coincidences becomes very long. An alternative method consists in fitting the total PL decay. Indeed, as mentioned before, the biexponential fit of the PL decay at 4 K gives values for the X* and BX* lifetimes in good agreement with the ones obtained from the ACF analysis. At RT, the fit of the PL decay rate [Fig. 3(d)] corresponding to the photons selected in the X* state [as in Fig. 2(b)] leads to a value of ∼1.5 ns for the BX* lifetime, that corresponds to $k_{BX^*}^{rad,RT} = 1/10\ ns^{-1}$ and $k_{BX^*}^{Auger,RT} = 1/1.8\ ns^{-1}$.

The typical QY, radiative and Auger lifetimes of BX* at 4 K and RT are summarized in Table I. First, one can notice that the Auger processes efficiency decreases by a factor of ∼2 between RT and 4 K. In strong contrast, the radiative lifetime is approximately four times reduced from RT to 4 K. In the case of the X* state,[27] a qualitatively similar behavior

TABLE I. QY, Auger, and radiative lifetimes of the BX* state at RT and 4 K.

	QY	Radiative lifetime (ns)	Auger lifetime (ns)
BX* (RT)	15%	10	1.8
BX* (4 K)	60%	2.5	3.8

was observed: the radiative lifetime decreases while Auger processes are completely suppressed. This was explained by the electron localization. At 300 K, a CdSe/CdS NC is a quasi-type II structure because the conduction-band offset (CBO) between CdSe and CdS is close to zero, that explains the long exciton lifetime (⩾60 ns). The results reported in Ref. 27 were consistent with a low conduction-band offset between CdSe and CdS of −50 meV at 200 K. At cryogenic temperature, the NC is a type I nanostructure and electrons are no longer delocalized in the whole CdSe/CdS structure but confined with the holes in the CdSe core. This confinement results in the decrease of the radiative lifetime of X*. However, since the electrons do not probe anymore the abrupt potential at the NC surface, the nonradiative Auger recombinations are inhibited even if the carrier confinement is highly enhanced. For X*, Auger recombinations are suppressed at 4 K while the radiative lifetime typically decreases from 30 ns to less than 10 ns from RT to 4 K.[27] The data of Table I first confirm the analysis made for the X* recombination. The table also shows that the radiative lifetime of BX* is four times lower at 4 K when compared to RT. However, compared to X*, Auger recombinations are still observed at 4 K for BX* (the peak at zero delay of the coincidence counts is always lower than the other ones). A likely explanation is that the wave function of the electron of BX* with the highest energy is slightly delocalized in the shell and probes the step potential at the NC surface.

C. Intensity fluctuations

While the thermal activation of the Auger process for the BX* state can be evidenced through the study of $g^2(\tau = 0)$ between RT and 4 K, the analysis of the ACF at positive delays leads to a full-comprehensive description of the intensity fluctuations of the X* state. Figure 4(a) represents the normalized area of the consecutive peaks of the ACF (the delay between each peak is equal to 400 ns at RT). For positive delays lower than 1 ms, the ACF is close to 1.1. This reflects an additional bunching of the fluorescence due to the switching of the NC fluorescence between gray and bright states at all these time scales. The value of the ACF is however close to 1 due to the low occurrence of gray periods and the high quantum efficiency of the gray state that induces a slightly low difference between the fluorescence intensity of bright and gray periods. Beyond 1 ms, the ACF decreases slowly to 1 and shows that no blinking occurs over a 10-ms time scale in agreement with a previous report.[2] These results are in strong contrast with the ones obtained for standard CdSe/ZnS NCs.[33] For these NCs, the deviation from the value of 1 of the ACF is much higher due to perfect extinction of the ionized NC. Moreover, the ACF decreases very slowly, falling abruptly to 1 at a time close to the measurement duration. It is worth

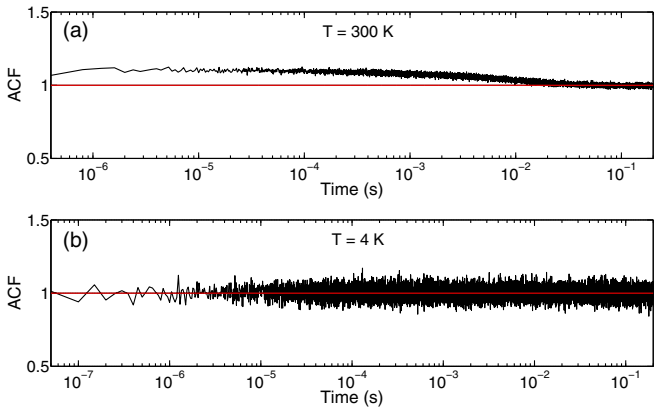

FIG. 4. (Color online) (a) Normalized area of the peaks of the autocorrelation function at 300 K. (b) Normalized area of the peaks of the autocorrelation function at 4 K.

noting that for CdSe/ZnS NCs the ACF also depends strongly on the considered time interval for the calculation. All these properties were related to the power-law statistics followed by the duration of the extinction periods[34] that is not observed for CdSe/CdS NCs.[2,35]

Even if the ACF remains close to 1, the slight deviation from unity has a strong impact in terms of intensity fluctuations. This can be illustrated through the Mandel factor $Q(T)$.[36,37] $Q(T)$ is defined as $\langle(\Delta N_T)^2\rangle/\langle N_T\rangle - 1$, where N is the photon number. The subscript T means that the standard deviation $\langle(\Delta N)^2\rangle$ and the average $\langle N\rangle$ are calculated for a number of photons detected over a measurement lasting T. $Q(T)$ evaluates the deviation from the Poissonian distribution of the number of photons detected during a time bin T, that constitutes the standard quantum limit and the shot-noise level. For a Poissonian statistics, $Q(T) = 0$, while for a perfect single-photon source $Q(T) = -1$. A value of $Q(T) > 0$ corresponds to a super-Poissonian distribution that is observed for a single emitter in case of flickering. $Q(T)$ is directly calculated by dividing the time trace in periods of duration T (chosen as a multiple of the laser repetition period) for which the number of detected photons is computed. Due to flickering, $Q(T)$ increases with T (Fig. 5). At short values of

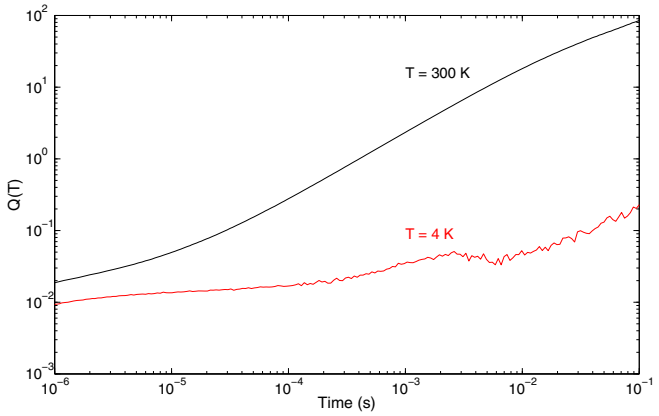

FIG. 5. (Color online) Mandel factor $Q(T)$ at 300 K (black line) and 4 K (red line).

T ($\leqslant 10\ \mu$s), $Q(T)$ increases relatively slowly due to the strong antibunching observed at zero delay that makes the stream of photons steady at short time scales. From $T = 10\ \mu$s to 10 ms, $Q(T)$ increases linearly. This can be understood through the equation directly linking $Q(T)$ to the ACF $g^{(2)}(\tau)$:[36,38]

$$Q(T) = \frac{\langle N_T\rangle}{T}\int_{-T}^{T}\left[1 - \frac{|\tau|}{T}\right](g^{(2)}(\tau) - 1)d\tau. \qquad (2)$$

This equation, valid under a continuous excitation, is a good approximation in our case when T is much larger than the period between the laser pulses. Since $g^{(2)}(\tau)$ is nearly constant between 10 μs and 10 ms, $Q(T)$ is a linear function of T. For higher values of T, $Q(T)$ increases more slowly due to the decrease of $g^{(2)}(\tau)$ at high values of τ. This behavior corresponds to the absence of long periods of low emission. However, for a time bin T of 10 ms (typical in intensity measurements), $Q(T)$ exceeds 80.

Under a low excitation, the ACF at 4 K is plotted in Fig. 4(b) for delays ranging from 50 ns to 200 ms. The unitary value of the ACF observed in Fig. 4(b) shows that no intensity fluctuations occur at time scales ranging from 50 ns (the repetition rate of the laser is now 20 MHz) to 200 ms. The NC is then ionized and the quantum efficiency of the trion state is perfectly stable and equal to 1 (the contribution of multiexcitonic states in the intensity emission is lower than 10% since the probability to excite the NC is here lower than 0.1). The two electrons and the hole of X* are confined in the core of the NC and the close environment of the NC does not influence the X* recombination. X* is a perfect and stable emitting state as the Auger effect is thermally suppressed. The absence of flickering at all time scales is also highlighted by the value of $Q(T)$ (Fig. 5) that remains very close to zero whatever the value of T (the slight increase at high T is due to the decrease of the number events used to calculate Q).

IV. CONCLUSION

In conclusion, the complete suppression of blinking at 4 K has been demonstrated through an analysis of the time statistics of the photons. While the recombination of X* is purely radiative, the QY of BX* is four times higher than at RT and up to 60%. A method of photon postselection is used to measure the rates involved in BX* recombinations. All these results enable us to understand in detail the modification with the temperature of the charge carrier confinement both for X* and BX*. Electrons and holes are highly localized in the core at 4 K. These results are a promising step for the synthesis of NC with a perfectly stable 100% fluorescence quantum yield at 300 K that be could be also used for lasing applications.

ACKNOWLEDGMENTS

This work has been supported by the Région Ile-de-France in the framework of DIM "des atomes froids aux nanosciences", and Institut Universitaire de France. B.D., L.B., and J.-P.H. also thank Agence Nationale de la Recherche (Grants No. Core-Shell ANR-08-BLAN-0034 and No. QDOTICS ANR-12-BS10-008), and Institut Universitaire de France for fundings. The authors thank L. Coolen for fruitful discussions.

*benoit.dubertret@espci.fr
†jean-pierre.hermier@uvsq.fr

[1] Y. F. Chen, J. Vela, H. Htoon, J. L. Casson, D. J. Werder, D. A. Bussian, V. I. Klimov, J. A. Hollingsworth, and Y. Chen, J. Am. Chem. Soc. **130**, 5026 (2008).
[2] B. Mahler, P. Spinicelli, S. Buil, X. Quélin, J.-P. Hermier, and B. Dubertret, Nat. Mat. **7**, 659 (2008).
[3] F. Cichos, C. von Borczyskowski, and M. Orrit, Curr. Opin. Colloid Interface Sci. **12**, 272 (2007).
[4] E. A. Riley, C. M. Hess, and P. J. Reid, Int. J. Mol. Sci. **13**, 12487 (2012).
[5] J. Zhao, G. Nair, B. R. Fisher, and M. G. Bawendi, Phys. Rev. Lett. **104**, 157403 (2010).
[6] P. A. Frantsuzov, S. Volkán-Kascó, and B. Jankó, Phys. Rev. Lett. **103**, 207402 (2009).
[7] P. A. Frantsunov, S. Volkán-Kascó, and B. Jankó, Nano Lett. **13**, 402 (2013).
[8] V. Klimov, A. Mihkailovsky, D. McBranch, C. Leatherdale, and M. Bawendi, Science **287**, 1011 (2000).
[9] Al. L. Efros and M. Rosen, Phys. Rev. Lett. **78**, 1110 (1997).
[10] F. Garcia-Santamara, Y. Chen, J. Vela, R. D. Schaller, J. A. Hollingsworth, and V. I. Klimov, Nano Lett. **9**, 3482 (2009).
[11] F. Garcia-Santamaria, S. Brovelli, R. Viswanatha, J. A. Hollingsworth, H. Htoon, S. Crooker, and V. I. Klimov, Nano Lett. **11**, 687 (2011).
[12] P. Spinicelli, S. Buil, X. Quélin, B. Mahler, B. Dubertret and J.-P. Hermier, Phys. Rev. Lett. **102**, 136801 (2009).
[13] R. Osovsky, D. Cheskis, V. Kloper, A. Sashchiuk, M. Kroner, and E. Lifshitz, Phys. Rev. Lett. **102**, 197401 (2009).
[14] X. Y. Wang, X. F. Ren, K. Kahen, M. A. Hahn, M. Rajeswaran, S. M. Zacher, J. Silcox, G. E. Cragg, A. L. Efros, and T. D. Krauss, Nature (London) **459**, 686 (2009).
[15] N. Amecke and F. Cichos, J. Lumin. **131**, 375 (2011).
[16] B. Lounis, H. A. Bechtel, D. Gerion, P. Alivisatos, and W. E. Moerner, Chem. Phys. Lett. **329**, 399 (2000).
[17] X. Brokmann, G. Messin, P. Desbiolles, E. Giacobino, M. Dahan, and J. P. Hermier, New J. Phys. **6**, 99 (2004).
[18] B. Fisher, J-M. Caruge, Y. T. Chan, J. E. Halpert, and M. Bawendi, Chem. Phys. **318**, 71 (2005).
[19] B. Fisher, J.-M. Caruge, D. Zehnder, and M. Bawendi, Phys. Rev. Lett. **94**, 087403 (2005).
[20] Y. S. Park, A. V. Malko, J. Vela, Y. Chen, Y. Ghosh, F. Garcia-Santamaria, J. A. Hollingsworth, V. I. Klimov, and H. Htoon, Phys. Rev. Lett. **106**, 187401 (2011).
[21] Y. Louyer, L. Biadala, J.-B. Trebbia, M. J. Fernée, Ph. Tamarat, and B. Lounis, Nano Lett. **11**, 4370 (2011).
[22] V. Klimov, A. Mikhailovsky, S. Xu, A. Malko, J. Hollingsworth, C. Leatherdale, and M. Bawendi, Science **290**, 314 (2000).
[23] L. W. Wang, M. Califano, A. Zunger, and A. Franceschetti, Phys. Rev. Lett. **91**, 056404 (2003).
[24] G. E. Cragg and A. L. Efros, Nano Lett. **10**, 313 (2010).
[25] D. Oron, M. Kazes, and U. Banin, Phys. Rev. B **75**, 035330 (2007).
[26] M. Zavelani-Rossi, M. G. Lupo, F. Tassone, L. Manna, and G. Lanzani, Nano Lett. **10**, 3142 (2010).
[27] C. Javaux, B. Mahler, B. Dubertret, A. Shabaev, A. V. Rodina, Al. L. Efros, D. R. Yakovlev, F. Liu, M. Bayer, G. Camps, L. Biadala, S. Buil, X. Quélin, and J.-P. Hermier, Nat. Nano. **8**, 206 (2013).
[28] M. J. Fernée, C. Sinito, Y. Louyer, C. Potzner, T. L. Nguyen, P. Mulvaney, P. Tamarat, and B. Lounis, Nat. Commun. **3**, 1287 (2012).
[29] A. Shabaev, A. V. Rodina and Al. L. Efros, Phys. Rev. B **86**, 205311 (2012).
[30] D. Canneson, I. Mallek-Zouari, S. Buil, X. Quélin, C. Javaux, B. Dubertret, and J.-P. Hermier, New J. Phys. **14**, 063035 (2012).
[31] D. Canneson, I. Mallek-Zouari, S. Buil, X. Quélin, C. Javaux, B. Mahler, B. Dubertret, and J.-P. Hermier, Phys. Rev. B **84**, 245423 (2011).
[32] G. Nair, L.-Y. Chang, S. M. Geyer, and M. Bawendi, Nano Lett. **11**, 1136 (2011).
[33] G. Messin, J. P. Hermier, E. Giacobino, P. Desbiolles, and M. Dahan, Opt. Lett. **26**, 1891 (2001).
[34] X. Brokmann, J. P. Hermier, G. Messin, P. Desbiolles, J. P. Bouchaud, and M. Dahan, Phys. Rev. Lett. **90**, 120601 (2003).
[35] O. Chen, J. Zhao, V. P. Chauhan, J. Cui, C. Wong, D. K. Harris, H. Wei, H.-S. Han, D. Fukumura, R. K. Jain, and M. G. Bawendi, Nat. Matter **12**, 445 (2013).
[36] L. Mandel, Opt. Lett. **4**, 205 (1979).
[37] F. Treussart, R. Alléaume, V. Le Floc'h, L. T. Xiao, J.-M. Courty, and J.-F. Roch, Phys. Rev. Lett. **89**, 093601 (2002).
[38] G. Messin, Habilitation à Diriger des Recherches, Université Paris Sud (2008).